Received: 9 June 2017 | Accepted: 26 June 2017

DOI: 10.1111/jace.15056

ORIGINAL ARTICLE

Journal of the American Ceramic Society

# $Ga_2S_3$-$Sb_2S_3$-CsI chalcohalide glasses for mid-infrared applications

**Jiahua Qiu[1] | Anping Yang[1] | Mingjie Zhang[1,2] | Lei Li[1] | Bin Zhang[1] | Dingyuan Tang[1] | Zhiyong Yang[1]**

[1]Jiangsu Key Laboratory of Advanced Laser Materials and Devices, School of Physics and Electronic Engineering, Jiangsu Normal University, Xuzhou, Jiangsu, China

[2]State Key Laboratory of Silicate Materials for Architectures, Wuhan University of Technology, Wuhan, Hubei, China

Correspondence
Anping Yang and Zhiyong Yang, Jiangsu Key Laboratory of Advanced Laser Materials and Devices, School of Physics and Electronic Engineering, Jiangsu Normal University, Xuzhou, Jiangsu, China

Emails: apyang@jsnu.edu.cn; yangzhiyong@jsnu.edu.cn

**Funding information**
Natural Science Foundation of Jiangsu Province, Grant/Award Number: BK20140239; Jiangsu Collaborative Innovation Centre of Advanced Laser Technology and Emerging Industry; Priority Academic Program Development of Jiangsu Higher Education Institutions; National Natural Science Foundation of China, Grant/Award Number: 61405080, 61205207, 61575086, 61405079

**Abstract**

In this study, a new chalcohalide glass system, $Ga_2S_3$-$Sb_2S_3$-CsI, is reported. It has a glass-forming domain composed of ~0-35 mol% $Ga_2S_3$, ~15-95 mol% $Sb_2S_3$, and ~0-55 mol% CsI. The glasses have a wide transparent window of ~0.7-13.5 μm, high third-order nonlinear refractive indices of ~1.7-8.7×$10^{-14}$ $cm^2$/W @ 1.55 μm, and relatively short zero group-velocity-dispersion wavelengths of 3.8-5.15 μm. The glasses can dissolve more than 2 mol% active ions (e.g., $Dy^{3+}$), and the doped glasses show intense emissions in the mid-infrared. These superior properties demonstrate their good potentials for mid-infrared applications such as thermal imaging, nonlinear photonics and lasers.

**KEYWORDS**
chalcogenide, fluorescence, glass forming, nonlinear photonics, optical property

## 1 | INTRODUCTION

Recently there have been growing demands for infrared (IR) optical materials because of the rapid advances in IR technology and extensive applications of IR devices.[1-3] Chalcogenide glasses (ChG), which are amorphous materials based on chalcogen elements (S, Se, and Te), are considered to be one of the most popular IR materials due to their advantages such as wide IR transparent window, excellent rheological property, and low cost.[4] Among ChG, sulfide glasses commonly show better mechanical properties than selenide or telluride ones owing to their stronger bond strength between constituent atoms, and therefore are favorable for practical applications. However, conventional sulfide glasses (e.g., Ge or As-based sulfides) can only transmit light up to ~10 μm. This makes them unfavorable for some applications which require the materials transmitting light with longer wavelength, typically up to ~12 μm in thermal imaging systems. The recently invented Ga-Sb-S glasses[5] showed outstanding transparency in the entire 1-12 μm spectral region thanks to their relatively low effective phonon energy, making it

  

possible to use robust sulfide glasses in thermal imaging systems. However, the glass-forming region of this chalcogenide system is quite small, which does not allow meaningful tuning of the composition or physical properties. In addition, it is difficult to prepare volume glass in a single ampoule because the glass is not stable enough against crystallization. Aiming to improve the glass forming ability and to extend the property tuning range while retaining the wide transparent window, the halide CsI is incorporated into the glass in this study, leading to a new chalcohalide system $Ga_2S_3$-$Sb_2S_3$-CsI. The glass forming region is determined, the properties are investigated, and the suitability of these glasses for mid-IR applications are assessed.

## 2 | EXPERIMENTAL PROCEDURE

The $Ga_2S_3$-$Sb_2S_3$-CsI glasses were synthesized by the conventional melt-quenching method.[6] About 10 g mixture of Ga (6N), Sb (6N), S (6N), and CsI (3N) were weighed and loaded into a clean quartz tube with an inner diameter of 9 mm and an outer diameter of 12 mm. The tube containing the mixture was then evacuated ($<10^{-5}$ torr) and sealed. The mixture was homogenized at 900°C for more than 12 hours in a rocking furnace. After that, the tube with the melt was quenched in water and the formed glass was annealed near the glass transition temperature ($T_g$) for 3 hours. The $Dy^{3+}$-doped $Ga_2S_3$-$Sb_2S_3$-CsI glasses were prepared by the same method. 3N $Dy_2S_3$ compound was used in the synthesis and the homogenizing temperature was 950°C.

To confirm the amorphous nature of the samples, X-ray diffraction (XRD, D2 Phaser, Bruker Corporation, Karlsruhe, Germany) measurements of the powders was conducted. The characteristic temperatures of the glasses were measured at a heating rate of 10°C/min using a Q2000 differential scanning calorimeter (DSC, TA Instruments, New Castle, DE). The densities ($d$) of the glasses were measured by the Archimede's method. The micro-hardness ($H_v$) tests were performed using a Q10A+ tester (Qness GmbH, Golling, Austria) under a load of 100 g for 5 second. The transmission spectra were recorded on double-side polished glass discs by a Lambda 950 spectrophotometer (Perkin-Elmer, Waltham, MA) in the 0.5-2.5 μm range and by a Tensor 27 Fourier transform infrared spectrophotometer (FTIR, Bruker, Ettlingen, Germany) in the 2.5-25 μm region. The linear refractive indices ($n_0$) were measured on single-side polished glass discs by an IR-VASE ellipsometer (J. A. Woollam, Lincoln, NE).[7,8] The third-order nonlinear refractive indices ($n_2$) and two-photon absorption (TPA) coefficients (β) at 1550 nm of the glasses were measured by the Z-Scan technique.[9] About 1.5 mm thick double-side-polished discs were used for the measurements. The mid-IR emission spectra of $Dy^{3+}$-doped glasses were measured using a FS980 fluorescence spectrometer (Edinburgh Instruments, Edinburgh, UK). The measurement scheme is similar to that described in Ref. [10]. All the measurements were carried out at room temperature.

## 3 | RESULTS AND DISCUSSION

The glass-forming region of $Ga_2S_3$-$Sb_2S_3$-CsI chalcogenide system is shown in Figure 1. The compositions consisting of 0-35% $Ga_2S_3$, 15-95 mol% $Sb_2S_3$, and 0-55% CsI can form glasses. The glass transition temperatures $T_g$ and the onset temperatures of crystallization ($T_x$) are determined from respective DSC curves and displayed in Table 1. The glasses have $T_g$ of 190-245°C. When the content of $Ga_2S_3$ or $Sb_2S_3$ is fixed (series A or C), the $T_g$ decreases with increasing CsI addition. When the amount of introduced CsI is fixed (series B), the $T_g$ increases with increasing $Ga_2S_3$ or decreasing $Sb_2S_3$ content. Apparently, when more than 20 mol% CsI is incorporated into $Ga_2S_3$-$Sb_2S_3$ system, the formed glasses exhibit relatively high $\Delta T$ ($=T_x-T_g$), indicating their good thermal stability against crystallization.

Table 2 lists measured physical parameters of the $Ga_2S_3$-$Sb_2S_3$-CsI glasses, and Figure 2 shows the transmission spectra of representative ones. The short-wavelength absorption edge $\lambda_S$ and the long-wavelength cut-off edge ($\lambda_L$) are defined as the wavelengths where the absorption coefficient is 10 $cm^{-1}$. These $Ga_2S_3$-$Sb_2S_3$-CsI glasses have $d$ of 3.78-3.97 $g/cm^3$, $\lambda_S$ of 586-713 nm, $\lambda_L$ of ~13.2-14.4 μm, $H_v$ of 125-188 $kg/mm^2$ and $n_0$ (@10 μm) of~2.01-2.58. When $Ga_2S_3$ content is fixed (series A), the $d$, $\lambda_S$, $H_v$, and $n_0$ decrease remarkably with increasing CsI

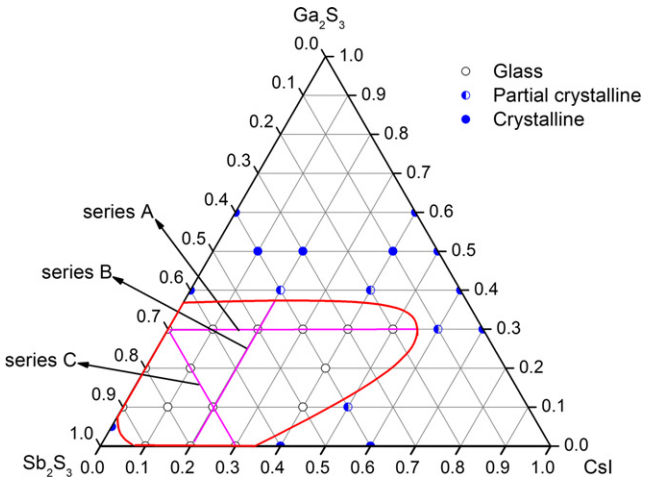


**FIGURE 1** Glass forming domain of $Ga_2S_3$-$Sb_2S_3$-CsI chalcohalide system obtained by quenching 10 g melts in water [Color figure can be viewed at wileyonlinelibrary.com]

**TABLE 1** Characteristic temperatures of $xGa_2S_3$-$ySb_2S_3$-zCsI glasses

| Category | x-y-z | $T_g$ (±1°C) | $T_x$ (±1°C) | $\Delta T$ (℃) |
|---|---|---|---|---|
| Series A | 30-70-0 | 245 | 329 | 84 |
| | 30-60-10 | 237 | 327 | 90 |
| | 30-50-20 | 235 | 338 | 103 |
| | 30-40-30 | 223 | 344 | 121 |
| | 30-30-40 | 214 | 347 | 133 |
| | 30-20-50 | 190 | 314 | 124 |
| Series B | 0-80-20 | 215 | 265 | 50 |
| | 10-70-20 | 217 | 323 | 106 |
| | 20-60-20 | 228 | 361 | 133 |
| | 30-50-20 | 235 | 338 | 103 |
| Series C | 30-70-0 | 245 | 329 | 84 |
| | 20-70-10 | 226 | 352 | 126 |
| | 10-70-20 | 217 | 323 | 106 |
| | 0-70-30 | 216 | 277 | 61 |

addition, but the $\lambda_L$ does not show an evident change. When CsI concentration is fixed (series B), the $d$, $\lambda_S$, $\lambda_L$, and $n_0$ decrease with increasing $Ga_2S_3$ content, whereas the $H_v$ shows an opposite trend. For the compositions containing the same amount of $Sb_2S_3$, with increasing CsI addition, the $d$ and $\lambda_L$ increase, while the $\lambda_S$, $H_v$, and $n_0$ decrease. In Figure 2, three absorption bands around 2.9 μm, 4.1 μm and 6.3 μm are evident. These bands are attributed to the absorptions of OH, SH, and $H_2O$ impurities, respectively.[11] The intensities of 2.9 μm and 6.3 μm bands increase significantly with increasing CsI addition because CsI is quite sensitive to moisture and it usually carries moisture as the starting material. Figure 2 also shows that the glasses exhibit relatively low transmittance in the 8.5-11.5 μm. This could be mainly caused by absorptions of oxygen-related impurities[11] (e.g., S-O, Ga-O). These impurities could be significantly reduced by further purification of the raw materials.

Table 3 shows the measured $n_2$ of the investigated glasses. The values of β are negligibly small (<0.01 cm/GW) and not listed in the table. These glasses have $n_2$ of $1.7\text{-}8.7\times10^{-14}$ $cm^2/W$, and it shows similar composition dependence to the $n_0$. This is consistent with the Miller's prediction, which indicates that a glass with a higher $n_0$ generally shows a higher $n_2$.[12]

$T_g$ of a glass is associated with the connectivity (degree of cross-linking) of the glass network and the average bond energy of the glass.[13] The former is expected to be the dominating factor in $Ga_2S_3$-$Sb_2S_3$-CsI glasses because the average bond energies of different compositions in this system are similar. Previous studies[5,9] imply that $Ga_2S_3$-$Sb_2S_3$ glasses have a three-dimensional continuous network structure consisting of crosslinked [$GaS_4$] tetrahedra, [$SbS_3$] pyramids and [$S_3Ga$-$GaS_3$] structural units (SU). After the addition of CsI, the Ga-Ga bonds in [$S_3Ga$-$GaS_3$] SU are supposed to break and the Ga atoms tend to capture I atoms to form Ga-I dangling bonds or [$GaS_{4-x}I_x$] SU.[14,15] The $Cs^+$ ions are likely to be located near the negatively charged [$GaS_{4-x}Cl_x$] SU and act as charge compensators. This will reduce the connectivity of the glass network, and therefore account for the decrease in the $T_g$ with increasing CsI addition in series A and series C glasses. When the addition of CsI is at the same level, more $Ga_2S_3$ is apt to

**TABLE 2** Densities ($d$), short-wavelength absorption edges ($\lambda_S$), long-wavelength cut-off edges ($\lambda_L$), micro-hardness ($H_v$) and linear refractive indices ($n_0$) of $xGa_2S_3$-$ySb_2S_3$-zCsI glasses

| Category | x-y-z | $d$ (g/cm$^3$) | $\lambda_s$ (nm) | $\lambda_L$ (μm) | $H_v$ (kg/mm$^2$) | $n_0$ (@10 μm) |
|---|---|---|---|---|---|---|
| Series A | 30-70-0 | 3.97 | 690 | 13.4 | 188 | 2.579 |
| | 30-60-10 | 3.93 | 668 | 13.4 | 171 | 2.464 |
| | 30-50-20 | 3.90 | 660 | 13.4 | 155 | 2.347 |
| | 30-40-30 | 3.85 | 624 | 13.3 | 152 | 2.226 |
| | 30-30-40 | 3.80 | 600 | 13.3 | 136 | 2.126 |
| | 30-20-50 | 3.78 | 586 | 13.2 | 125 | 2.015 |
| Series B | 0-80-20 | 4.14 | 713 | 14.3 | 128 | 2.557 |
| | 10-70-20 | 4.05 | 679 | 14.0 | 131 | 2.478 |
| | 20-60-20 | 3.97 | 665 | 13.7 | 142 | 2.406 |
| | 30-50-20 | 3.90 | 660 | 13.4 | 155 | 2.347 |
| Series C | 30-70-0 | 3.97 | 690 | 13.4 | 188 | 2.579 |
| | 20-70-10 | 4.00 | 683 | 13.7 | 151 | 2.524 |
| | 10-70-20 | 4.05 | 679 | 14.0 | 131 | 2.478 |
| | 0-70-30 | 4.10 | 675 | 14.4 | 127 | 2.455 |

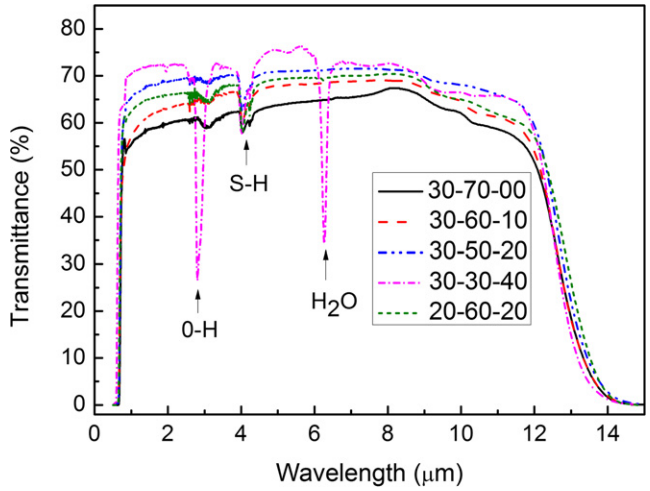


**FIGURE 2** Transmission spectra of $xGa_2S_3$-$ySb_2S_3$-zCsI glasses (the thickness is 2 mm) [Color figure can be viewed at wileyonlinelibrary.com]

**TABLE 3** Linear refractive indices ($n_0$), third-order nonlinear refractive indices ($n_2$), and zero dispersion wavelength ($\lambda_0$) for $xGa_2S_3$-$ySb_2S_3$-zCsI glasses

| *x*-y-z | $n_0$ (@1550 nm) | $n_2$ ($10^{-14}$ cm$^2$/W) | $\lambda_0$ (μm) |
|---|---|---|---|
| 30-70-0 | 2.684 | 8.7 | 5.15 |
| 30-60-10 | 2.542 | 5.9 | 4.58 |
| 30-50-20 | 2.415 | 3.8 | 4.41 |
| 30-40-30 | 2.274 | 2.7 | 3.96 |
| 30-30-40 | 2.181 | 1.7 | 3.80 |
| 0-80-20 | 2.626 | 7.3 | 4.57 |
| 10-70-20 | 2.538 | 5.8 | 4.42 |
| 20-60-20 | 2.474 | 4.8 | 4.23 |
| 20-70-10 | 2.604 | 7.0 | 4.79 |
| 0-70-30 | 2.511 | 5.4 | 3.84 |

increase the connectivity of the glass network because Ga is four-coordinated but Sb is three-coordinated. This could explain the increase in $T_g$ with increasing $Ga_2S_3$ content in series B glasses. In chalcogenide glasses, the connectivity of the glass network and the average bond energy of the glass usually also dominate $H_v$ of the glass.[16] This is consistent with the similar composition dependence of $H_v$ and $T_g$, as shown in Tables 1 and 2.

$\lambda_S$ of a glass can be qualitatively estimated from an empirical formula[6,17]:

$$\frac{hc}{\lambda_s} \propto \chi + w - \varphi \tag{1}$$

where $h$ is Planck's constant, $c$ is the speed of light in vacuum, $\chi$ is average electron affinity of anions, $w$ is average bond energy of the glass, and $\varphi$ is average polarization energy of constituent atoms. I has higher electronegativity than S, and the polarizability follows the order of Cs<Ga<Sb and I<S.[18] Considering $w$ does not change remarkably, the value of $(\chi+w-\varphi)$ increases with increasing CsI concentration in the series A and series C glasses. This explains the decrease in $\lambda_S$ with increasing CsI addition. For the series B glasses where the CsI concentration is fixed, the higher polarizability of Sb than Ga makes the glass containing more $Ga_2S_3$ show smaller $\lambda_S$.

$\lambda_L$ of a glass is related to its effective phonon energy (EPE).[19] When $Sb_2S_3$ is substituted by CsI, the glass network will contain more I atoms and less Sb atoms. Thus, the EPE is not expected to change evidently because I and Sb have similar atomic mass. This may explain the minimal change in the $\lambda_L$ in series A glasses. When $Ga_2S_3$ is replaced by $Sb_2S_3$ (or CsI), the glass network will contain more heavy atoms (e.g., Sb or I). This will lead to the decrease in EPE, and therefore result in larger $\lambda_L$. This is consistent with the variation in $\lambda_L$ in series B and series C glasses.

$n_0$ of a glass is related to the electric polarizability ($p$) of constituent elements and density $d$ of the glass.[8,20,21] Its value could be estimated according to the following equation.

$$n^2 = \frac{2\sum_i R_i x_i + \frac{M}{d}}{\frac{M}{d} - \sum_i R_i x_i} \tag{2}$$

where $R_i = p_i/K$ ($K$ is a constant), is the molar refractivity of the constituent element, $x_i$ is the molar percentage of the element with the $R_i$ (or $p_i$), and $M$ is the molar mass of the glass. When CsI is added into $Ga_2S_3$-$Sb_2S_3$ glasses, the formation of Ga-I dangling bonds makes the structure more open, leading to lower $d$. This is in agreement with the decrease in the $d$ with increasing CsI addition in series A glasses. Because Sb and Ga have higher $p$ than Cs, and S have higher $p$ than I, the average $p$ decreases with increasing CsI addition for this series of glasses. Thus, the simultaneous decreases of $d$ and average $p$ with increasing CsI addition lead to the decrease in the $n_0$. For the glasses in series B, as discussed above, the glass containing more $Ga_2S_3$ exhibits higher connectivity or lower compactness of the network when CsI content is fixed. Besides, Ga has lower atomic mass than Sb. These two factors make the $d$ decrease with increasing $Ga_2S_3$ content in this series of glasses (see Table 2). Furthermore, with increasing $Ga_2S_3$ content, the average $p$ also decreases due to the lower $p$ of Ga compared to Sb. The decreases of the $d$ and average $p$ with increasing $Ga_2S_3$ content result in the decrease in the $n_0$ for this series of glasses. For the glasses in series C, although the structure becomes more open with increasing CsI addition, the $d$ still increases due to the much higher average atomic mass of CsI than $Ga_2S_3$. The $n_0$ shows an opposite composition dependence to the $d$ in this series of

glasses probably because of the much lower molar refractivity ($R$) of CsI than $Ga_2S_3$.

The $Ga_2S_3$-$Sb_2S_3$-CsI glasses show good transmittance (>54%) in the whole 1-12 μm spectral range, suggesting that these glasses could be good optical materials for IR imaging. Some of the glasses exhibit excellent thermal stability against crystallization. This is favorable for producing volume high-quality or complex optical elements. In addition, the relatively large glass-forming region of this chalcohalide system makes it feasible to tune the glass properties according to practical requirements. One may worry that the glasses will be inevitably attacked by moisture in the applications. To avoid this attack, protecting layers[22,23] could be coated on the surface of the glasses.

The high $n_2$ and negligible β of $Ga_2S_3$-$Sb_2S_3$-CsI glasses in addition to their good IR transparency indicate that these glasses could also be good materials for IR optical nonlinear applications such as all-optical switching and supercontinuum (SC) generation. Recently, SC generation in the mid-IR is one of the hot research topics in materials sciences and nonlinear photonics.[24–27] To achieve high-brightness broadband mid-IR SC in a chalcogenide waveguide, the waveguide is supposed to be pumped with short laser pulses at its anomalous group velocity dispersion (GVD) region.[24-26] Thus, a base glass with zero GVD at relatively short wavelength is desirable, because it is relatively easy to shift the zero GVD wavelength ($\lambda_0$) of a designed waveguide to a shorter wavelength where an affordable efficient pump laser is available. The $\lambda_0$ of the $Ga_2S_3$-$Sb_2S_3$-CsI glasses are calculated and displayed in Table 3. They are shorter than those of Ga-Sb-S glasses,[5] and the value becomes smaller with increasing CsI content. This makes these glasses more suitable for nonlinear photonics.

The long $\lambda_L$ of the $Ga_2S_3$-$Sb_2S_3$-CsI glasses imply that they have low EPEs. Hence, the glasses doped with active ions (AIs) are expected to be good IR gain media. We found that the glasses could dissolve more than 2 mol% $Dy^{3+}$ ions without deteriorating the glass transparency. Figure 3 shows an emission spectrum of 0.2 mol% $Dy^{3+}$-doped $20Ga_2S_3$-$60Sb_2S_3$-20CsI glass when exited at 1320 nm. Intense emissions around 2.95 μm and 4.40 μm were observed, and the measured fluorescence lifetimes were ~3.28 ms and 1.24 ms, respectively. Spectral analyses indicate that the quantum efficiencies of the 2.95 μm and 4.40 μm emissions were 86% and 72%, respectively. These superior emission properties demonstrate good potential of the $Ga_2S_3$-$Sb_2S_3$-CsI glasses as host materials for AI dopants.

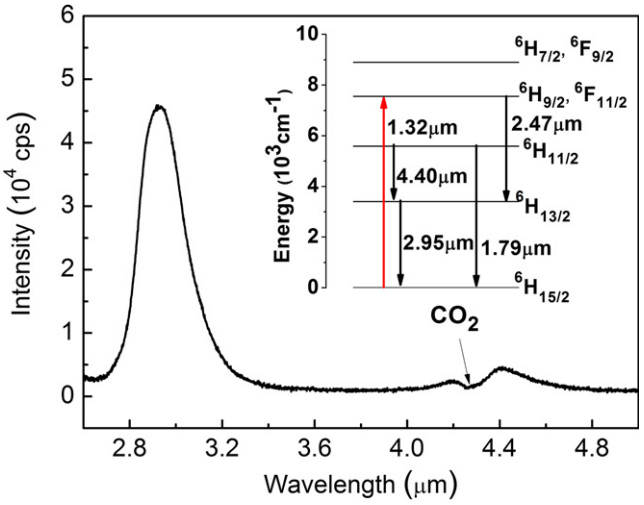


**FIGURE 3** Emission spectrum of 0.2 mol% $Dy^{3+}$-doped $20Ga_2S_3$-$60Sb_2S_3$-20CsI glass when excited at 1320 nm. The inset is a diagram of energy levels of $Dy^{3+}$ ions with possible transitions [Color figure can be viewed at wileyonlinelibrary.com]

## 4 | CONCLUSIONS

Up to 55 mol% CsI can be incorporated into $Ga_2S_3$-$Sb_2S_3$ chalcogenide system to form a glass, leading to a relatively large glass forming region of the resulting $Ga_2S_3$-$Sb_2S_3$-CsI chalcohalide system. These glasses have $T_g$ of 190-245°C, $d$ of 3.78-3.97 g/cm$^3$, $\lambda_S$ of 586-713 nm, $\lambda_L$ of ~13.2-14.4 μm, $H_v$ of 125-188 kg/mm$^2$, and $n_0$ (@10 μm) of~2.01-2.58. They show good transmittance in the whole 1-12 μm range, high $n_2$ (1.7-8.7×10$^{-14}$ cm$^2$/W @ 1550 nm), negligible small β, and relatively short $\lambda_0$ (3.8-5.15 μm). They can dissolve more than 2 mol% $Dy^{3+}$ ions, and the doped glasses show intense mid-IR emissions with high quantum efficiencies. These superior properties make the $Ga_2S_3$-$Sb_2S_3$-CsI glasses good candidate materials for mid-IR applications such as thermal imaging, nonlinear photonics, and lasers.

## ACKNOWLEDGEMENTS

This work was supported by the National Natural Science Foundation of China (61405080, 61205207, 61575086, 61405079), the Natural Science Foundation of Jiangsu Province (BK20140239), the Priority Academic Program Development of Jiangsu Higher Education Institutions, and Jiangsu Collaborative Innovation Centre of Advanced Laser Technology and Emerging Industry.

## REFERENCES

1. Kimber JA, Foreman L, Turner B, et al. FTIR spectroscopic imaging and mapping with correcting lenses for studies of biological cells and tissues. *Faraday Discuss*. 2016;187:69-85.
2. Kim W, Nguyen V, Shaw L, et al. Recent progress in chalcogenide fiber technology at NRL. *J Non-Cryst Solids*. 2016;431:8-15.
3. Lucas P, Coleman G, Cantoni C, et al. Chalcogenide glass sensors for bio-molecule detection. *Proc SPIE*. 2017;10058:100580Q, (15 pp).

4. Hilton AR. *Chalcogenide glasses for infrared optics*. New York, NY: McGraw-Hill; 2010.
5. Yang AP, Zhang MJ, Li L, et al. Ga-Sb-S chalcogenide glasses for mid-infrared applications. *J Am Ceram Soc*. 2016;99:12-15.
6. Yang ZY, Luo L, Chen W. Red color $GeSe_2$-based chalcohalide glasses for infrared optics. *J Am Ceram Soc*. 2006;89:2327-2329.
7. Woollam J, Johs B, Herzinger C, et al. Overview of variable-angle spectroscopic ellipsometry (VASE): I. Basic theory and typical applications. *Proc SPIE*. 1999; CR72:3-28.
8. Yang Y, Yang ZY, Lucas P, et al. Composition dependence of physical and optical properties in Ge-As-S chalcogenide glasses. *J Non-Cryst Solids*. 2016;440:38-42.
9. Zhang MJ, Yang ZY, Li L, et al. The effects of germanium addition on properties of Ga-Sb-S chalcogenide glasses. *J Non-Cryst Solids*. 2016;452:114-118.
10. Zhang MJ, Yang AP, Peng YF, et al. $Dy^{3+}$-doped Ga-Sb-S chalcogenide glasses for mid-infrared lasers. *Mater Res Bull*. 2015;70:55-59.
11. Snopatin G, Shiryaev V, Plotnichenko V, et al. High-purity chalcogenide glasses for fiber optics. *Inorg Mater*. 2009;45:1439-1460.
12. Boyd RW. *Nonlinear optics*. San Diego, CA: Academic Press; 2003.
13. Tichý L, Tichá H. Covalent bond approach to the glass-transition temperature of chalcogenide glasses. *J Non-Cryst Solids*. 1995;189:141-146.
14. Song JH, Choi YG, Heo J. Ge and Ga K-edge EXAFS analyses on the structure of Ge-Ga-S-CsBr glasses. *J Non-Cryst Solids*. 2006;352:423-428.
15. Lin CG, Qu G, Li Z, et al. Correlation between crystallization behavior and network structure in $GeS_2$-$Ga_2S_3$-CsI chalcogenide glasses. *J Am Ceram Soc*. 2013;96:1779-1782.
16. Feltz A. *Amorphous inorganic materials and glasses*. Weinheim: VCH; 1993.
17. Cui M. *Glass technology*. Beijing: Light Industry Press; 1987.
18. Yue Y, Zhu R. *Inorganic chemistry (5th edition)*. Beijing: Higer Education Press; 2006.
19. Nakamoto K. *Infrared and raman spectra of inorganic and coordination compounds, part A: Theory and applications in inorganic chemistry (6th edition)*. Hoboken: Wiley; 2008.
20. Wang YW, Qi SS, Yang ZY, et al. Composition dependences of refractive index and thermo-optic coefficient in Ge-As-Se chalcogenide glasses. *J Non-Cryst Solids*. 2017;459:88-93.
21. Gleason B, Richardson K, Sisken L, et al. Refractive index and thermo-optic coefficients of Ge-As-Se chalcogenide glasses. *Int J Appl Glass Sci*. 2016;7:374-383.
22. Kutsay O, Gontar A, Novikov N, et al. Diamond-like carbon films in multilayered interference coatings for IR optical elements. *Diamond Relat Mater*. 2001;10:1846-1849.
23. Bréhault A, Calvez L, Adam P, et al. Moldable multispectral glasses in $GeS_2$-$Ga_2S_3$-CsCl system transparent from the visible up to the thermal infrared regions. *J Non-Cryst Solids*. 2016;431:25-30.
24. Petersen C, Møller U, Kubat I, et al. Mid-infrared supercontinuum covering the 1.4-13.3 μm molecular fingerprint region usingultrahigh NA chalcogenide step-index fibre. *Nat Photon*. 2014;8:830-834.
25. Yu Y, Gai X, Ma P, et al. Experimental demonstration of linearly polarized 2-10 μm supercontinuum generation in a chalcogenide rib waveguide. *Opt Lett*. 2016;41:958-961.
26. Zhang B, Yu Y, Zhai CC, et al. High brightness 2.2-12 μm mid-infrared supercontinuum generation in a nontoxic chalcogenide step-index fiber. *J Am Ceram Soc*. 2016;99:2565-2568.
27. Zhao Z, Wu B, Wang X, et al. Mid-infrared supercontinuum covering 2.0-16 μm in a low-loss telluride single-mode fiber. *Laser Photonics Rev*. 2007;11:1700005. (6 pp)


**How to cite this article:** Qiu J, Yang A, Zhang M, et al. $Ga_2S_3$-$Sb_2S_3$-CsI chalcohalide glasses for mid-infrared applications. *J Am Ceram Soc*. 2017;100:5107–5112. https://doi.org/10.1111/jace.15056